Available on CMS information server

CMS CR -2016/289

The Compact Muon Solenoid Experiment

Conference Report

Mailing address: CMS CERN, CH-1211 GENEVA 23, Switzerland

27 October 2016 (v2, 01 November 2016)

Study of the performance of RPC system installed at the CMS experiment

M. Shopova, R. Hadjiiska on behalf of the CMS muon group

Abstract

The CMS (Compact Muon Solenoid) experiment is a general purpose detector, located at the CERN Large Hadron Collider (LHC). It has a muon spectrometer equipped with a redundant system composed of three different detector technologies - Resistive Plate Chambers (RPCs) and Drift Tubes (DTs) in the barrel and RPC and Cathode Strip Chambers (CSCs) in the endcap region. All three are used for muon reconstruction and triggering. The RPC detector system consists of a total of 1056 double-gap chambers, covering the pseudo-rapidity region up to eta below 1.6. Here are presented the Resistive Plate Chambers performance results for the period of 2015 and 2016 with pp collisions at 13 TeV. The stability of the RPC performance is reported in terms of efficiency, cluster size and rate distributions.

Presented at *3rdPhysBulgaria Third National Congress On Physical Sciences*

Study of the performance of RPC system installed at the CMS experiment

M. Shopova[a*], R. Hadjiiska[a*]
On behalf of the CMS muon group

[a] *Bulgarian Academy of Sciences, Inst. for Nucl. Res. and Nucl. Energy, Tzarigradsko shaussee Boulevard 72, BG-1784 Sofia, Bulgaria.*

E-mail: mariana.vutova@cern.ch; roumyana.mileva.hadjiiska@cern.ch

ABSTRACT: The CMS (Compact Muon Solenoid) experiment is a general purpose detector, located at the CERN Large Hadron Collider (LHC). It has a muon spectrometer equipped with a redundant system composed of three different detector technologies – Resistive Plate Chambers (RPCs) and Drift Tubes (DTs) in the barrel and RPC and Cathode Strip Chambers (CSCs) in the endcap region. All three are used for muon reconstruction and triggering. The RPC detector system consists of a total of 1056 double-gap chambers, covering the pseudo-rapidity region up to $|\eta| \leq 1.6$. Here are presented the Resistive Plate Chambers performance results for the period of 2015 and 2016 with pp collisions at 13 TeV. The stability of the RPC performance is reported in terms of efficiency, cluster size and rate distributions.

KEYWORDS: Resistive-plate Chambers, Muon spectrometers.

[*] Corresponding author.

Contents

1. Instroduction

The Compact Muon Solenoid (CMS) [1] is a multipurpose detector operating at the Large Hadron Collider (LHC) at CERN, which has been successfully collecting data since the start of the first physics run period in 2009. It has a redundant and robust muon system [2] which uses three different gaseous detector technologies – Drift Tubes (DTs) in the barrel region, Cathode Strip Chambers (CSCs) in the endcap region and Resistive Plate Chambers (RPCs) both in barrel and endcap regions. The RPC system consists of 1056 detectors which cover an active area of more than 3500 m^2. The barrel region is cylindrical and has 4 stations, which are grouped into 5 wheels around the beam pipe, while the endcap region is planar and has 4 stations called disks. During the first long shutdown (LS1) of the LHC (2013 - 2014), the CMS muon upgrade collaboration added 144 new double-gap RPC detectors, thus completing the 4th forward stations (RE4s) [3]. Adding these stations increased the overall robustness of the CMS muon spectrometer and improved the trigger efficiency in the endcap region with pseudorapidity in the range $1.2 < |\eta| < 1.6$, shown in Fig. 1.

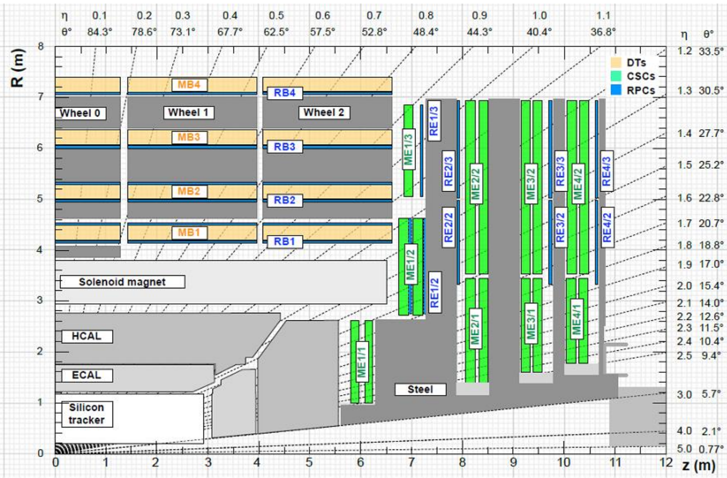

Figure 1. Longitudinal layout of one quadrant of the CMS detector which shows the enhancement in trigger efficiency with 4th endcap (RE4) in the pseudorapidity region $1.2 < |\eta| < 1.6$.

2. Chamber design and performance

The RPC chambers rely on 2 mm High Pressure Laminate (HPL) gas gaps, organized in a double-layer configuration with a copper strip readout panel placed in between. The HPL sheets resistivity is of the order of 2 – 5*10^{10} Ωcm. They operate in avalanche mode with a standard gas mixture of 95.2% $C_2H_2F_4$, 4.5% iC_4H_{10} and 0.3% SF_6.

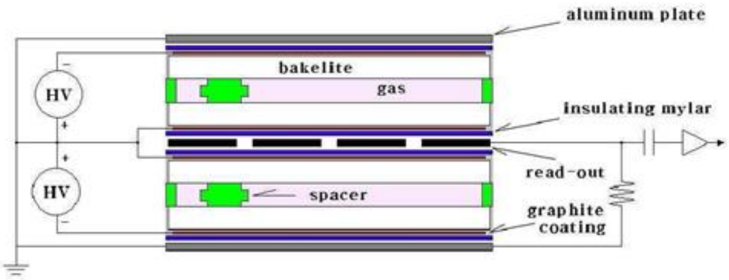

Figure 2. Schematic representation of the double gap layout of the RPC chambers.

The RPC chambers are subdivided in 2 or 3 η-partitions called rolls. [4]. The readout strips have different geometry depending on which part of the system they are in – the barrel chambers have rectangular shaped strips, while in the endcap chambers their shape is trapezoidal. This geometry difference is driven by the need to have adjustable trigger on different pT muons. The pitch of the strips depends on the distance to the beam pipe varying from 1.5 cm for the innermost stations to 4 cm for the outermost stations.

2.1 Efficiency

The efficiency of the RPC detectors strongly depends on the applied high voltage. The nominal operation high voltage for each chamber is called Working Point. In order to determine the best Working Point for each chamber, High Voltage scans are performed [4].

The RPC efficiency is calculated as the ratio between the number of detected and the number of expected hits. Expected hits are defined using a segment extrapolation method [5], [6]. Standalone muon tracks are reconstructed without taking into account RPC hits in order to avoid biases. Segments (DT in the Barrel and CSC in the endcap) that belong to a standalone muon track are selected and extrapolated to the plane of a given RPC. The detector unit is considered efficient if an RPC reconstructed hit is found within ± 2 strips from the position extrapolated from the DT/CSC segment.

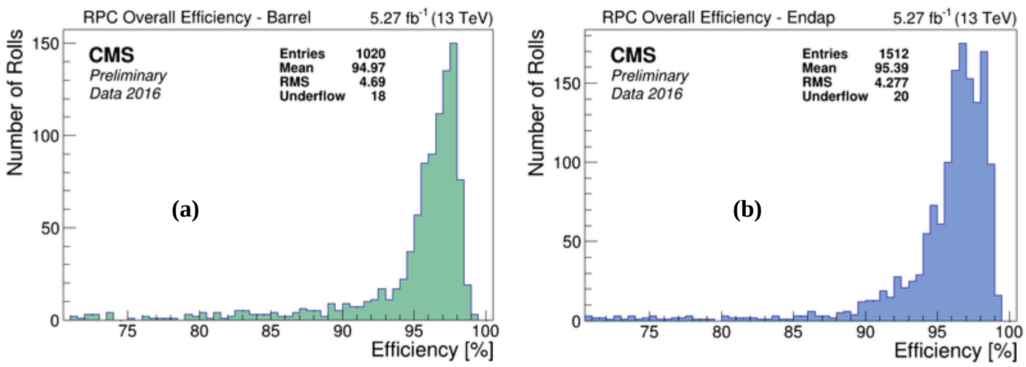

Figure 3. Overall efficiency for the barrel region (a) and the endcap region (b) estimated for 2016 data taken at 3.8 Tesla.

The overall efficiency distribution for both parts of the RPC system is shown in Fig.3. It is based on the analysis with proton-proton collision data at sqrt(s) = 13 TeV.

The underflow entries in the plots are from rolls with efficiency lower than 70%, caused by the known hardware problems – chambers with gas leak problems in the barrel and low voltage problems in the endcap. These rolls are 1.8% of all barrel rolls and 1.2% of all endcap rolls.

2.2 Cluster size

An important quantity defining the RPC spatial resolution is the cluster size. The RPC cluster size is defined as the number of adjacent strips fired simultaneously. Fig. 4 shows an example of a 2-dimensional plot representing the mean value of the cluster size distribution for every particular RPC eta partition (RPC roll) for one of the Endcap stations. The X axis corresponds to the sector numbers. There are 36 sectors per ring in the endcap stations and every sector covers 10° in azimuthal direction. The Y axis corresponds to the ring number and the RPC eta partition's names. The rolls installed at lower eta are shown on the top of the plot, while the rolls at higher eta (closest to the beam pipe) are shown on the lower part of the plot. The cluster size depends on the strip pitch and because of this it is higher for the innermost eta partitions (Ring 2, Rolls C) and it is smaller for the outermost ones (Ring 3, Rolls A).

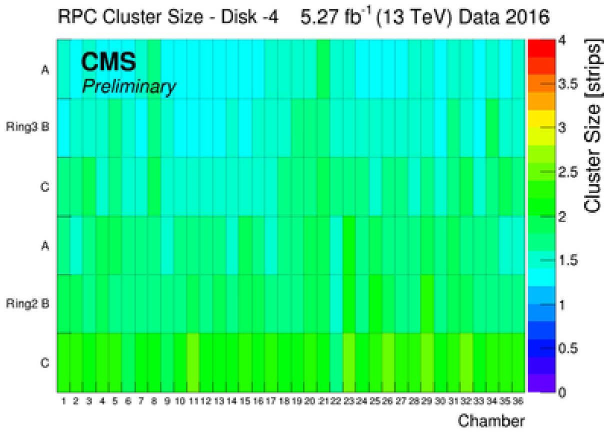

Figure 4. 2D map of the RPC cluster size for each roll of endcap disk RE-4.

The mean value for the RPC system cluster size is < 2 strips as it can be seen from Fig. 5, where the summary for the cluster size for all barrel and endcap rolls is shown.

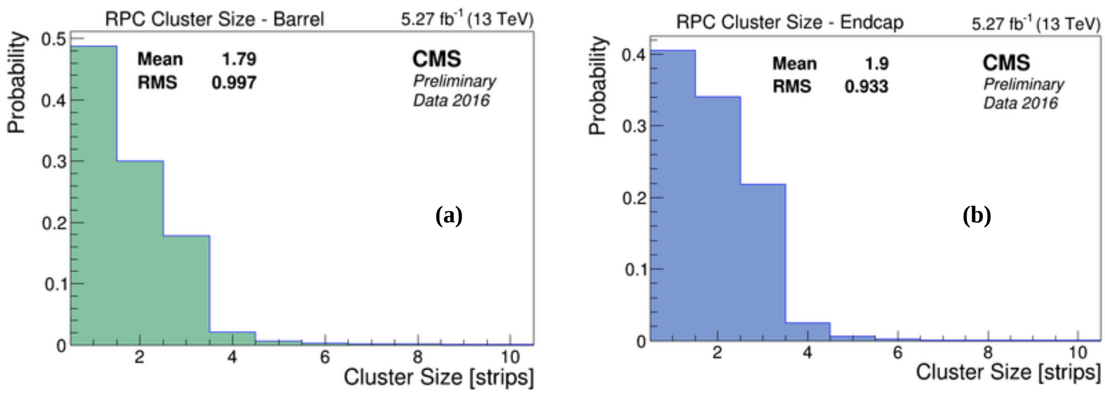

Figure 5. Summary plot of the RPC cluster size for all barrel rolls (a) and all endcap rolls (b).

2.3 Spacial resolution

The segment extrapolation method also allows the estimation of the RPC spatial resolution. Residuals are calculated as the distance in local x coordinates (transverse view at the RPC detection plane) between the extrapolated point and the center of the matched RPC reconstructed cluster. Plots given in Fig. 6 show the residual distributions for all RPC barrel layers.

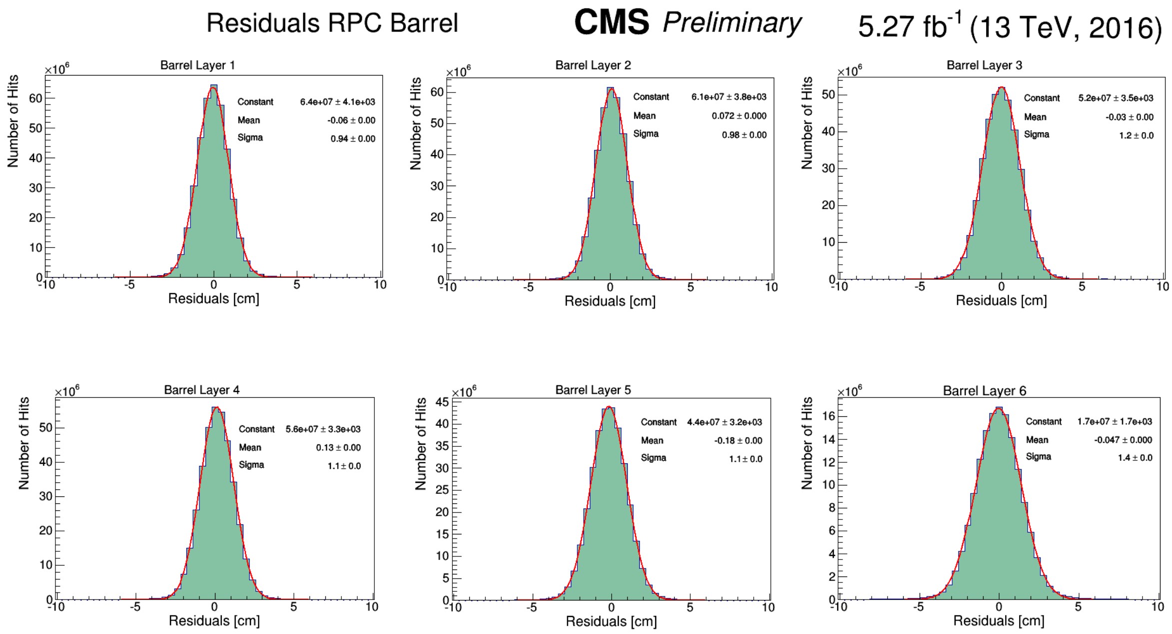

Figure 6. Residuals for all barrel layers. The order of the layers is such that layer 1 is the closest to the beam pipe, while layer 6 is the farthest from it.

The residual distributions have been fit to Gaussian distributions and the resulting mean and σ are given on each plot. The obtained σs are in agreement with the expectations [2].

2.4 RPC Background

The overall performance of the CMS RPC system depends also on the background radiation levels as it gives the main contribution in the measured RPC rate. Fig. 7 shows the approximately linear increase of the RPC rates with the increase of the LHC luminosity.

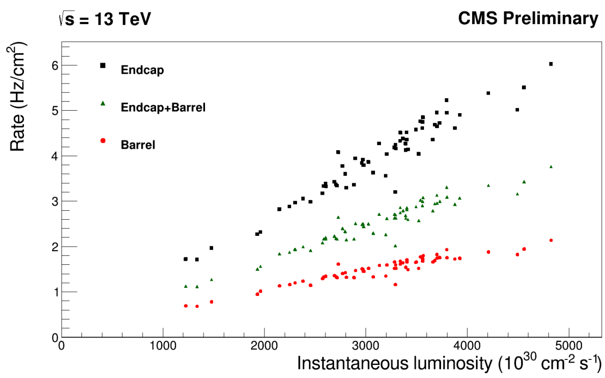

Figure 7. Average hit rate vs. instantaneous luminosity, with 2015 13TeV pp collisions data.

The red dots represent the rate measured in barrel and the black represent the rate measured in endcap. The green markers relate to the overall rate evaluated for the entire RPC system. It can be easily seen that rates increase for those chambers which are farther from the interaction point.

3. Conclusions

During the 2015-2016 data taking, the CMS RPC system is operating very well and stable. The quality of the experimental data taken, as well as the performance of the system is in agreement with expectations and simulations with average efficiency of ~95%, average cluster size persistently below 2 and average rate of < 5Hz/cm^2.

Acknowledgments

The authors would like to thank everyone in the CERN accelerator departments for the excellent performance of the LHC machine. We would also like to thank our colleagues from the CMS muon system and the RPC collaboration. We would also like to acknowledge the enduring support for the construction and operation of the LHC and the CMS detector provided by the following funding agencies: BMWFW and FWF (Austria); FNRS and FWO (Belgium); CNPq, CAPES, FAPERJ, and FAPESP (Brazil); MES (Bulgaria); CERN; CAS, MoST and NSFC (China); COLCIENCIAS (Colombia); MSES and CSF (Croatia); RPF (Cyprus); SENESCYT (Ecuador); MoER, ERC IUT and ERDF (Estonia); Academy of Finland, MEC, and HIP (Finland); CEA and CNRS/IN2P3 (France); BMBF, DFG, and HGF (Germany); GSRT (Greece); OTKA and NIH (Hungary); DAE and DST (India); IPM (Iran); SFI (Ireland); INFN (Italy); MSIP and NRF (Republic of Korea); LAS (Lithuania); MOE and UM (Malaysia); BUAP, CINVESTAV, CONACYT, LNS, SEP, and UASLP-FAI (Mexico); MBIE (New Zealand); PAEC (Pakistan); MSHE and NSC (Poland); FCT (Portugal); JINR (Dubna); MON, RosAtom, RAS and RFBR (Russia); MESTD (Serbia); SEIDI and CPAN (Spain); Swiss Funding Agencies (Switzerland); MST (Taipei); ThEPCenter, IPST, STAR and NSTDA (Thailand); TUBITAK and TAEK (Turkey); NASU and SFFR (Ukraine); STFC (United Kingdom); DOE and NSF (USA). Support for this research was given by Bulgarian Academy of Sciences under contract No. DCERN 01/02. **This research has also been funded by the Program for Supporting of Young Scientists, Bulgarian Academy of Sciences under contract No. DFNP-45.**

References

[1] CMS collaboration, “The CMS experiment at the CERN LHC,” JINST 3, S08004 (2008).

[2] CMS collaboration, *The Muon Project, CMS Technical Design Report,* CERN/LHCC 97-32, CMS-TDR-003.

[3] S. Colafranceschi et al., *Resistive Plate Chambers for 2013-2014 muon upgrade in CMS at LHC,* 2014 *JINST* **9** C10033.

[4] M. Abbrescia et al., *Cosmic ray test of double-gap resistive plate chambers for the CMS experiment,* Nucl. Instr. Meth. A.550 (2005) 116.

[5] “The performance of the CMS muon detector in proton-proton collisions at sqrt(s) = 7 TeV at the LHC”, CMS-MUO-11-001, 2013 *JINST* **8** P11002.

[6] CMS Collaboration, “Performance study of the CMS barrel resistive plate chambers with cosmic rays”, JINST 5 (2010) T03017.